



Pontrelli, G., Toniolo, G., McGinty, S., Peri, D., Succi, S. and Chatgialoglu, C. (2021) Mathematical modelling of drug delivery from pH-responsive nanocontainers. *Computers in Biology and Medicine*, 131, 104238.

(doi: [10.1016/j.combiomed.2021.104238](https://doi.org/10.1016/j.combiomed.2021.104238))

This is the Author Accepted Manuscript.

There may be differences between this version and the published version. You are advised to consult the publisher's version if you wish to cite from it.

<https://eprints.gla.ac.uk/229031/>

Deposited on: 20 January 2021

Mathematical modelling of drug delivery from pH-responsive nanocontainers

G. Pontrelli^{1,**}, G. Toniolo^{2,3}, S. McGinty⁴, D. Peri¹, S. Succi⁵, C. Chatgililoglu²

Abstract

Targeted drug delivery systems represent a promising strategy to treat localised disease with minimum impact on the surrounding tissue. In particular, polymeric nanocontainers have attracted major interest because of their structural and morphological advantages and the variety of polymers that can be used, allowing the synthesis of materials capable of responding to the biochemical alterations of the environment. While experimental methodologies can provide much insight, the generation of experimental data across a wide parameter space is usually prohibitively time consuming and/or expensive. To better understand the influence of varying design parameters on the release profile and drug kinetics involved, appropriately-designed mathematical models are of great benefit. Here, we developed a continuum-scale mathematical model to describe drug transport within, and release from, a hollow nanocontainer consisting of a core and a pH-responsive polymeric shell. Our two-layer mathematical model accounts for drug dissolution and diffusion and includes a mechanism to account for trapping of drug molecules within the shell. We conduct a sensitivity analysis to assess the effect of varying the model parameters on the overall behaviour of the system. To demonstrate the **usefulness** of our model, we focus on the particular case of cancer treatment and calibrate the model against release profile data for two anti-cancer therapeutical agents. We show that the model is capable of capturing the experimentally observed pH-dependent release.

Keywords: Drug release, nanocontainers, pH-responsive systems, mathematical model, parametric **identification, optimization**, numerical methods.

1. Introduction

The use of micro- and nano-particles as drug delivery systems (DDSs) is an extensive area of research, but the full potential of such technology has yet to be realised. There is growing interest in utilizing hydrogels, polymeric microspheres and nanoparticles as carrier systems for

*Corresponding author: Email address: giuseppe.pontrelli@gmail.com.

**Corresponding author: Email address: giuseppe.pontrelli@gmail.com.

¹Istituto per le Applicazioni del Calcolo – CNR Via dei Taurini 19, Rome, Italy

²ISOF-CNR, Via P. Gobetti 101, Bologna, Italy

³Institute of Nanoscience and Nanotechnology, N.C.S.R. Demokritos, 15310 Agia Paraskevi Attikis, Greece

⁴Division of Biomedical Engineering, University of Glasgow, Glasgow, UK.

⁵Italian Institute of Technology, CLNS@SAPIENZA, Roma, Italy

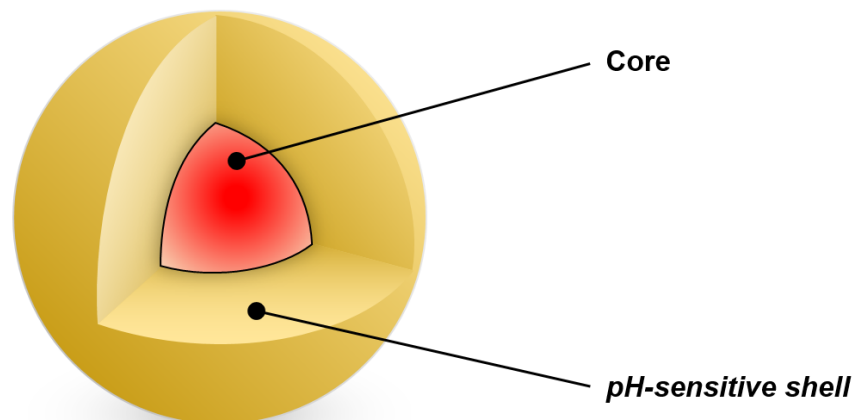


Figure 1: 3D representation of a core-shell nanocontainer (figure not to scale).

cell-specific targeting and for ‘smart’ delivery, with potential advantages including the reduction in systemic side-effects and an increase in drug efficacy [1-9]. The effectiveness of nanoscale polymeric delivery systems can be improved by designing structures capable of responding to specific pre-set conditions by altering their properties and favoring the release of the loaded drug. Stimuli-responsive nanocontainers (NC) are a family of DDSs that can control the release of the therapeutic active agents in response to external triggers **and stimuli** such as temperature, pH and many others [10]. They are considered to have potential applications in many areas such as drug delivery, because of the ability to release their contents in a desired and controlled manner. In particular, when the pore geometry is altered in response to environmental stimuli, such as pH, the NC changes its permeability making the controlled release of the cargo possible, thereby providing a wide range of bio-applications [3]. Therefore, the development of new kinds of environmental stimuli-responsive and smart DDSs is relevant and highly desirable. They have gained increasing attention recently and many examples can be found in literature [4, 9, 11, 12, 13]. Since their inception, nanoscale DDSs have represented one of the most promising strategies to efficiently treat cancer and to overcome the unpleasant side-effects of conventional chemotherapy [14, 15]. The efficacy of cancer drugs is limited in clinical administration due to their toxicity and poor solubility. Moreover, intravenous injection and infusion are associated with considerable fluctuations of drug concentration in the blood. Therefore, drugs can only be administered over a low dosage and a limited period of time. This is the underlying reason for the employment of pH-sensitive DDSs as amelioration for cancer therapy, since it takes advantage of the unique features to direct the drug to its target [16, 17, 18, 19].

Typically, a core-shell NC consists of a drug-loaded (fluid or solid) spherical centre (core) coated by a polymeric layer (shell) acting as a protective barrier against external chemical aggression and mechanical erosion. The core structure is generally conceived to locate the therapeutic agent, whilst the polymer shell is designed to control the release (fig. 1). The drug is encapsulated in both compartments but the core is known to be extremely important to increase the amount of

loaded drug compared to other systems [20]. Such two-layer assembly allows for better control of the drug release.

Mathematical and computational (*in silico*) modelling can provide a better understanding of the influence of different design parameters, which may then either be used to reduce the number of experiments or, more ambitiously, as a predictive screening tool for drug carriers [21]. Mathematical models in this field are typically empirical/semi-empirical or mechanistic. The former usually results in relatively simple equations that facilitate use for experimental scientists. Since the pioneering work of Higuchi [22], many empirical and semi-empirical models have been developed through the decades. Such models typically establish a simple power-law relationship between drug release and time, with the exponent being indicative of the release mechanism (e.g. diffusion, swelling, non-Fickian diffusion or erosion) [23, 24]. The alternative approach, which has been gaining increasing momentum, is the development of fully mechanistic continuum models, accounting for various phenomenon through more complicated physics-based equations and involving parameters with a direct physical and chemical meaning [8, 25, 26]. Each approach has its own benefits, challenges and limitations. However, theoretical studies on drug delivery from pH-responsive systems are relatively scarce. One exception is the work of Manga et al. [6], who considered the effect of pH on drug release from hydrogels by modelling a pH-dependent swelling behaviour.

In this paper, we develop a continuum-scale mathematical model of drug transport within, and release from, a drug-loaded NC. The model considers the two distinct layers (core and shell) and accounts for drug dissolution and diffusion within the core, as well as diffusion and a drug retention mechanism within the shell. Several of the model parameters are considered pH-dependent, enabling the model to account for pH-dependent release. We conduct a sensitivity analysis to assess the effect of varying the model parameters on the overall behaviour of the system. To demonstrate the utility of our model, we focus on the particular case of cancer treatment and calibrate the model against release profile data for two chemicals, daunorubicin and $[\text{Cu}(\text{TPMA})(\text{Phenantroline})](\text{ClO}_4)_2$. We show that the model, when all parameters are correctly identified through an optimization procedure, is capable of capturing the observed pH-dependent release.

2. The mathematical model

2.1. Modelling drug release from core-shell nanocontainers

We consider a single NC as a two-layer spherical system, comprising an internal core Ω_0 and the enveloping concentric polymeric shell Ω_1 (core-shell NC). Let us denote by R_0 and R_1 the internal and external radius of the NC, with the origin located at the centre of the NC and the r -axis oriented with the positive direction pointing outwards (fig. 2). In what follows, the subscripts 0 and 1 indicate parameters and variables referring to the core and shell layer, respectively. Assuming homogeneity and isotropy of each layer, we can assume that net drug diffusion occurs along the radial direction only, and thus we restrict our study to a one-dimensional model that reflects a perfectly radially symmetric system.

The majority of the drug is contained within the core, and we assume an initially homogeneous distribution within this region, at some concentration B_0 . However, the particle preparation meth-

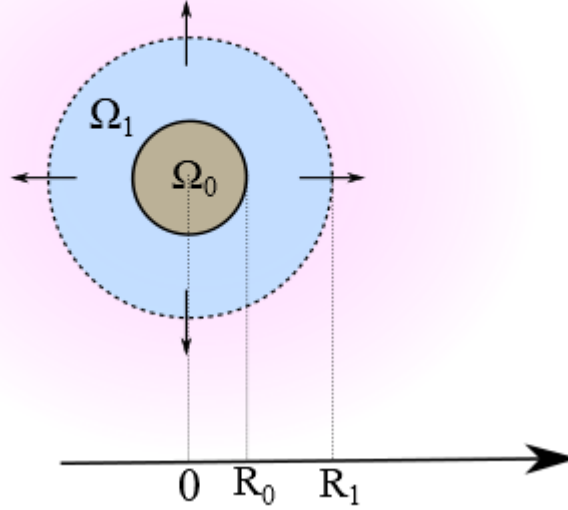


Figure 2: Schematic representation of a cross-section of the two-layer NC, comprising an internal core Ω_0 and an external shell Ω_1 (figure not to scale).

ods may also result in some drug mass being contained with the shell initially (see sect. S.1–S.2). We assume that this drug, of concentration B_1 , is permanently encapsulated and will never be released. When exposed to the release medium, the NC uptakes water and a dissolution process ensues in the permeated core, converting immobile (undissolved) drug of concentration $b_0(r, t)$ in the core to dissolved drug of concentration $c_0(r, t)$. Following our previous work [27], we model dissolution as a nonlinear process whereby drug in the core dissolves at a rate β and in proportion to the difference between the dissolved drug concentration and the solubility S in the medium. When dissolved, the drug is able to diffuse through the core with diffusion coefficient D_0 . The dynamics of drug dissolution and diffusion in Ω_0 is then described by the following two nonlinear partial differential equations:

$$\begin{aligned} \frac{\partial b_0}{\partial t} &= -\beta b_0^{2/3} (S - c_0), \\ \frac{\partial c_0}{\partial t} &= D_0 \left(\frac{\partial^2 c_0}{\partial r^2} + \frac{2}{r} \frac{\partial c_0}{\partial r} \right) + \beta b_0^{2/3} (S - c_0), \quad \text{in } (0, R_0). \end{aligned} \quad (2.1)$$

The $2/3$ exponent accounts for potential influences on the dissolution rate as the surface area of the dissolving drug particles change [28].

Let us now model the drug kinetics in the shell Ω_1 . Experimental evidence clearly shows that a pH-dependent fraction of the initial drug loading is typically retained and is never released

[12]. We model this observed phenomenon through a first order reaction kinetics, whereby drug diffusing through the polymeric shell has the possibility to permanently bind to the polymeric shell at a rate k [27]. We note that other forms of reaction could have been considered: in this study, however, we chose to focus on a simple linear reaction model in the absence of evidence to suggest otherwise. Denoting by $b_1(r, t)$ and $c_1(r, t)$ the bound and unbound phase concentrations, respectively, the drug dynamics in Ω_1 is then governed by the following equations [27]:

$$\begin{aligned}\frac{\partial c_1}{\partial t} &= D_1 \left(\frac{\partial^2 c_1}{\partial r^2} + \frac{2}{r} \frac{\partial c_1}{\partial r} \right) - kc_1 \\ \frac{\partial b_1}{\partial t} &= kc_1 \quad \text{in } (R_0, R_1),\end{aligned}\tag{2.2}$$

where D_1 represents the diffusion coefficient in the shell.

To close the system (2.1)–(2.2), we are required to impose appropriate boundary and initial conditions. At the interface between the core and shell layers, we assume continuity of flux and concentration:

$$-D_0 \frac{\partial c_0}{\partial r} = -D_1 \frac{\partial c_1}{\partial r}, \quad c_0 = c_1 \quad \text{at } r = R_0.\tag{2.3}$$

For radial symmetry we require:

$$\frac{\partial c_0}{\partial r} = 0 \quad \text{at } r = 0.\tag{2.4}$$

At the NC surface, we impose a perfect sink condition, reflecting the typical conditions of *in vitro* experiments considering these systems:

$$c_1 = 0, \quad \text{at } r = R_1,\tag{2.5}$$

At initial time, the drug is loaded in the core at concentration B_0 , while the shell contains bound drug at concentration B_1 :

$$b_0 = B_0, \quad c_0 = 0 \quad b_1 = B_1 \quad c_1 = 0\tag{2.6}$$

The total mass of drug within the NC at any time is given by integrating the concentration of each phase and layer over the corresponding volume [27], that is

$$M_{tot}(t) = 4\pi \left[\int_0^{R_0} r^2 \{b_0(r, t) + c_0(r, t)\} dr + \int_{R_0}^{R_1} r^2 \{b_1(r, t) + c_1(r, t)\} dr \right]\tag{2.7}$$

The release profile, $M_{rel}(t)$, defined as the cumulative % of drug released by time t , is then given by

$$\%M_{rel}(t) = \frac{M_{tot}(0) - M_{tot}(t)}{M_{tot}(0)} \times 100,\tag{2.8}$$

where $M_{tot}(0)$ is the total initial mass of drug in the NC. For convenience, we summarize the variables and parameters of the model in Table 1.

Table 1: Parameters and variables of the model

Parameter	Name	Units
r	radial coordinate	cm
c, b	free, bound drug concentration	$mol\ cm^{-3}$
R_0, R_1	internal, external radius	cm
D_0, D_1	drug diffusivity in Ω_0, Ω_1	$cm^2\ s^{-1}$
β	dissolution rate	$s^{-1}(mol\ cm^{-3})^{-2/3}$
S	solubility limit	$mol\ cm^{-3}$
k	drug-polymer reaction rate	s^{-1}
B_0, B_1	Initial concentration in Ω_0, Ω_1	$mol\ cm^{-3}$

2.2. Model solution method

Before solving the model (2.1)–(2.6) numerically, it is convenient first to nondimensionalise the equations. We scale r with the radius of the shell and scale t with the timescale for diffusion in the shell:

$$r \rightarrow \frac{r}{R_1}, \quad t \rightarrow \frac{D_1}{R_1^2} t. \quad (2.9)$$

Scaling all concentrations with B_0 , the model may be written in terms of five non-dimensional groups:

$$D = \frac{D_0}{D_1}, \quad Da = \frac{\beta B_0^{2/3} R_1^2}{D_1}, \quad \tilde{k} = \frac{k R_1^2}{D_1}, \quad \tilde{S} = \frac{S}{B_0}, \quad \tilde{B}_1 = \frac{B_1}{B_0}, \quad (2.10)$$

where Da may be regarded as a Damköhler number, defined as the ratio of dissolution rate to diffusion rate, and \tilde{k} denotes the ratio between the binding rate and rate of diffusion in the shell.

Summarizing, the nondimensional model is given by:

$$\frac{\partial b_0}{\partial t} = -Da b_0^{2/3} (\tilde{S} - c_0) \quad \text{in } (0, R_0), \quad (2.11)$$

$$\frac{\partial c_0}{\partial t} = D \left(\frac{\partial^2 c_0}{\partial r^2} + \frac{2}{r} \frac{\partial c_0}{\partial r} \right) + Da b_0^{2/3} (\tilde{S} - c_0), \quad \text{in } (0, R_0), \quad (2.12)$$

$$\frac{\partial c_1}{\partial t} = \frac{\partial^2 c_1}{\partial r^2} + \frac{2}{r} \frac{\partial c_1}{\partial r} - \tilde{k} c_1 \quad \text{in } (R_0, 1), \quad (2.13)$$

$$\frac{\partial b_1}{\partial t} = \tilde{k} c_1 \quad \text{in } (R_0, 1), \quad (2.14)$$

$$\frac{\partial c_0}{\partial r} = 0 \quad \text{at } r = 0, \quad (2.15)$$

$$-D \frac{\partial c_0}{\partial r} = -\frac{\partial c_1}{\partial r}, \quad c_0 = c_1 \quad \text{at } r = R_0, \quad (2.16)$$

$$c_1 = 0, \quad \text{at } r = 1. \quad (2.17)$$

We proceed to solve the system of equations (2.11)-(2.17) numerically, building on the method we described previously [27]. Let us subdivide the interval $(0, R_0)$ into $N + 1$ equispaced grid nodes, and the interval $(R_0, 1)$ into $M + 1$ equispaced points, with h_0 and h_1 the spacing in the core and shell layers, respectively. Let us indicate by a superscript j the approximated value of the concentrations at r_j . In each layer, we approximate the diffusive terms by considering a standard second order central difference in space of the second derivative at internal nodes. The reaction terms in eqn. (2.11) and (2.14) do not contain any spatial derivatives and therefore are evaluated pointwise. For example, (2.12) is discretized at node r_j as:

$$\left. \frac{dc_0}{dt} \right|_{r_j} = D \frac{c_0^{j-1} - 2c_0^j + c_0^{j+1}}{h_0^2} + Da (b_0^j)^{2/3} (\tilde{S} - c_0^j). \quad (2.18)$$

After spatial discretization, the system of PDEs reduces to a set of nonlinear ordinary differential eqns. of the form:

$$\frac{dY}{dt} = A(Y), \quad (2.19)$$

where $Y = (b_0^0, \dots, b_0^{N-1}, c_0^0, \dots, c_0^{N-1}, c_1^1, \dots, c_1^M, b_1^1, \dots, b_1^M)^T$ and $A(Y)$ contains the discretized eqns. (2.11)-(2.14) and related boundary/interface conditions (2.15)-(2.17). The ODE system (2.19) is solved by the routine `ode15s` of `Matlab` based on a Runge-Kutta type method with backward differentiation formulas, and an adaptive time step [27]. To validate the computational scheme, we have performed a number of checks which give confidence in our numerical results. In particular we have verified the second order degree of accuracy against an analytically solvable diffusion model in composite media [29].

2.3. Parameter identification methodology

As in many biological systems, the model contains a number of interdependent parameters: most of them are not known *a priori*, and for those parameters of which estimates do exist, these are often subject to high variability and uncertainty. Obtaining reliable estimates of parameters is a significant challenge in the field. Starting from a wide range of physically realistic parameters, we address this issue here in two steps. Firstly, we perform a sensitivity analysis on four key dimensionless parameters, D , Da , \tilde{S} and \tilde{k} , to evaluate the sensitivity of the results to changes in these parameters (see section 3.1). Then, by comparison with experimental data sets, we inversely estimate the non-dimensional parameters for the specific systems considered. Specifically, using the experimental values, we inversely estimate the five unknown nondimensional parameters (2.10) for each pH considered, such that the model solution best fits the data set.

The experimental data are compared with the predictions of the numerical model, and the parameters are used as independent variables to minimize the distance between the experimental data and the numerical prediction. An optimization problem is then formulated as follows: given N_s experimental samples $X_i = X(t_i)$ (cumulative % of drug released) measured at different times t_i , we define our objective function by a least squares method:

$$F(\xi) = \sum_{i=1}^{N_s} (X_i - x_i(\xi))^2$$

where $x_i(\xi)$ correspond to the computed quantities, depending on the unknown parameter set ξ . Then, we minimize F subject to a number of constraints and ξ in a given range. However, due to the high variability of the space of parameters, some combinations are physically unrealistic, and consequently lead to unphysical results that should be discarded. To address this point, two different constraint functions are adopted here. The first **stipulates** that the mass of drug released cannot be negative, and the second ensures the positiveness of the first derivative of the drug release curve, since a negative value would imply that released drug re-enters the NC. Unfortunately, the space of the parameters ξ is very large: this poses some further difficulties in the optimization problem, increasing also the number of areas where the design parameters produce good values of $F(\xi)$. Taking account of the aforementioned challenges, we devised an ad hoc algorithm as described below.

For each pH we have a different target curve to fit, so that we need to solve different optimization problems. This results in a set of five optimal design parameters for each experimental dataset. Nonetheless, we note that the parameter \tilde{B}_1 , **(the ratio between the initial drug concentration in the shell and in the core, see eqn (2.10))**, does not depend on pH. In order to identify the value of \tilde{B}_1 , we split the optimization process in two steps. In the first step, \tilde{B}_1 is considered in the same way as the other parameters. A sensible range is defined for the five parameters (2.10) (table 2) and a global optimization process is performed. The adopted search algorithm is the Parameter Space Investigation (PSI) [30]: some sample configurations are uniformly distributed into the variable space. The uniformity of the distribution of samples is very important since, at the beginning, every part of the variable space has the same probability to contain the global optimum. The search is then concentrated in the neighborhood of the current best configuration. In order to reduce the number of samples preserving the uniformity of the search, a Uniformly Distributed Sequence is adopted [31] for the selection of the candidates. This class of distribution is designed to produce a sequence of **equispaced** points. The search is executed in parallel, so that the overall computational time is further reduced. Due to the wide range of parameters, they are uniformly distributed over a logarithmic scale: in this way, their order of magnitude is more easily **identified**. We use a relatively high number (1024) of samples **(not changed along the iterations)** to avoid that certain basins of attraction are neglected. Once all the configurations have been computed, the successive area of investigation is represented by the subspace including the five best locations previously detected. The use of more than a single point is suggested because at the initial stage of the search we have a rather crude estimate of the variable space, so that one could be distracted by a local minimizer that cannot be further improved, discarding the basin of attraction of the global minimum. This procedure is repeated ten times, providing a successive refinement of the feasible area.

In the second step, the average of \tilde{B}_1 over pH is selected and kept fixed and the optimization procedure with a pattern-search algorithm [32] is used to refine the remaining four values at each pH.

Table 2: Possible range of the nondimensional parameters considered in the optimization algorithm. These ranges were chosen based on physical constraints and typical values, and span at least 3 orders of magnitude for each parameter.

Parameter	Min.	Max.
D	2	10^3
Da	10^{-2}	10^2
\tilde{S}	10^{-2}	10^2
\tilde{k}	10^{-2}	10^2
\tilde{B}_1	10^{-3}	10

3. Results and discussion

3.1. Sensitivity analysis

The **present** problem depends on five nondimensional parameters, whose interrelatedness dictates that they should vary in a finite range, to ensure physical compatibility. We start by performing a sensitivity analysis on the four non-dimensional parameters D , Da , \tilde{S} and \tilde{k} . We fix $R_0 = 0.5$ and $\tilde{B}_1 = 0.1$ and we vary the other parameters one at a time from the baseline case where we set $D = 100$, $Da = 0.1$, $\tilde{k} = 1$ and $\tilde{S} = 1$.

We first investigate the variation in the release profile with changes to the diffusivity ratio D (fig. 3, top left). For $D \geq 1$, meaning that the diffusion coefficient in the core is greater or equal to that of the shell, the drug release profile remains almost unchanged because the release is limited by the relatively slow transport through the shell. However, as we decrease D , the transport is hindered by the drug's reduced ability to diffuse through the core and as such the drug release is slowed down. In particular, we see a change in concavity in the drug release profile at early times, representing a delay in release as a result of the increased time to diffuse through the core. Interestingly, we also observe that D has an influence on the mass of drug retained within the shell. Specifically, reducing D results in less drug being permanently bound (more drug released overall). The explanation for this is that the retention is dependent not only on the binding rate within the shell, but also on the spatio-temporal drug concentration. As D is reduced, the free drug concentration in the shell is also reduced at any given time, meaning that less drug becomes permanently bound.

Figure 3 (top right) demonstrates that \tilde{k} predominantly affects the drug retention capacity of the NC. As \tilde{k} is increased, more drug is retained within the polymeric shell and is never released, with the release rate also reduced. Conversely, increasing Da leads to a faster drug release rate, driven by an increased rate of dissolution relative to diffusion. As Da is increased, the time taken for **the** complete release of non-retained drug is reduced (fig. 3 bottom left). The influence of \tilde{S} (fig. 3 bottom right) in the dissolution term is similar to that of Da , though they are related to different physical mechanisms. This explorative sensitivity analysis confirms the correct behaviour of the model under a number of different parameter regimes.

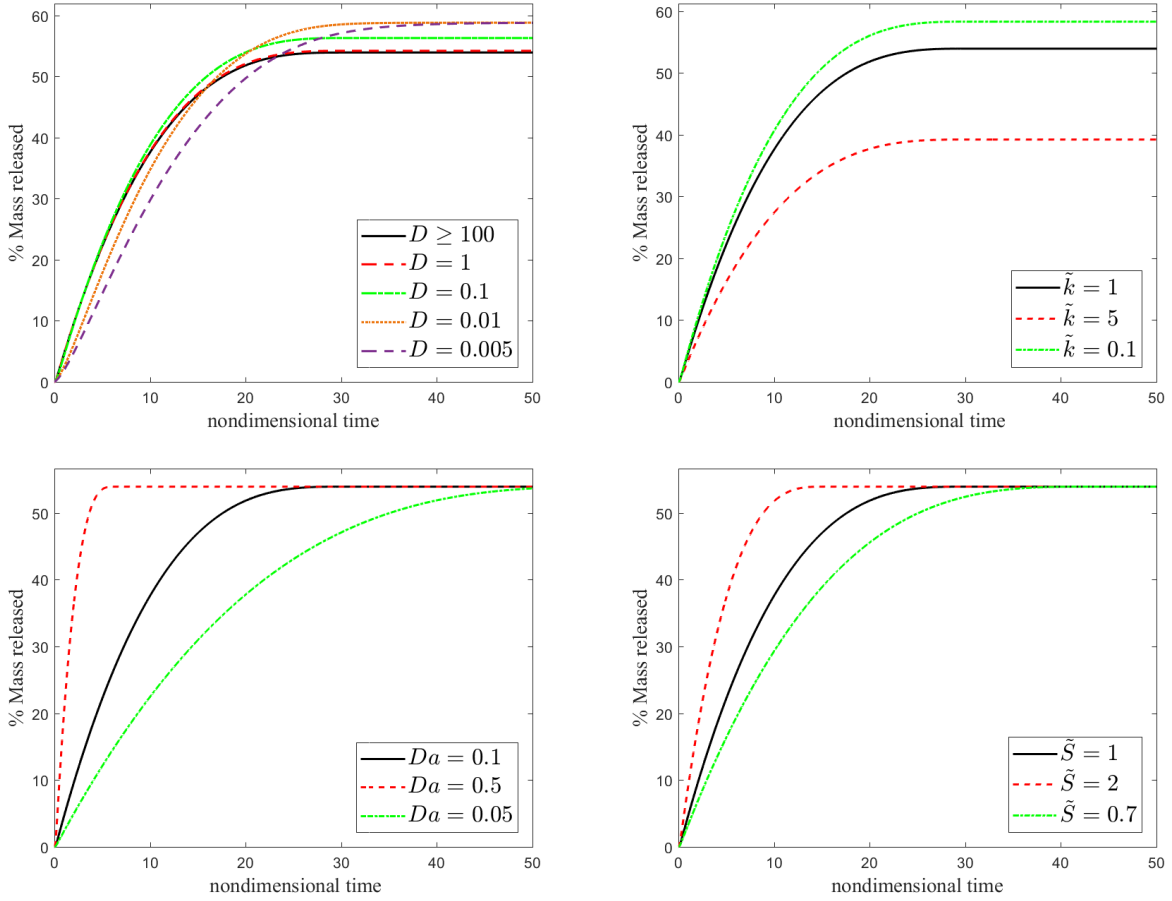


Figure 3: Variation in % cumulative mass released versus nondimensional time when D , \tilde{k} , Da and \tilde{S} are changed over the baseline case.

3.2. Case study

NCs are able to target **tumoral tissues** because of the enhanced penetration and retention effect [20]. This is a peculiar feature of solid tumours, based on their anatomical and physiopathological characteristics, such as large gaps in the newly-formed blood vessels, which result in leaky and inefficient lymphatic drainage, allowing NCs to remain and accumulate in the tumor site. A DDS with a size compatible with the gaps in the tumour blood vessel can exploit the enhanced penetration and retention effect and selectively target the tumoral tissue. NCs enter the cell via the endosome-lysosome system, the preferential route for the internalization [35].

Besides the aforementioned properties, tumor cells and tissues are characterized by some internal biochemical alterations that can be used as a trigger for drug release [33, 34]. Among these alterations, the best known and most exploited one is probably pH. There is a clear difference between healthy tissues (pH \approx 7.4) and diseased tissues (pH $<$ 6.0 in tumours). Also, intracellular differences between normal and cancer cells have been highlighted and can be used to facilitate drug delivery [4, 18]. At a tissue level, tumours have lower extracellular pH due to their faster metabolism and lower oxygen content. Lack of oxygen may cause hypoxia, leading to the produc-

tion of lactic acid, which in turn reduces pH in the tissue [34]. In particular, when DDSs enter the tumour cells via the endosome-lysosome system, they encounter a much lower pH than in healthy cells: lysosomal pH in cancer has been reported to be as low as 4.0 [35].

In this case study, we consider experimental data sets comprising drug release profiles of pH-sensitive NCs containing two molecules: (i) the chemotherapeutic agent daunorubicin (DNR) and (ii) $[\text{Cu}(\text{TPMA})(\text{Phenantroline})](\text{ClO}_4)_2$ (CTP), a highly innovative metallodrug recently documented for gene therapy [12, 36]. DNR is currently one of the most used chemotherapy agents while CTP is a very promising candidate for future generation medicine which would greatly benefit from selective release in the target area. Our goal is to calibrate the model using these data sets to demonstrate that the model we have presented is able to capture the drug release. Specifically, we aim at demonstrating that our model can capture two important features of these systems, i.e. the pH-responsive release and the drug retention effect.

3.2.1. DNR and CTP *in vitro* drug release

Our previous study on CTP release from NCs revealed that the amount of delivered drug varies depending on the pH of the environment [12]. The CTP release profile from the NCs was studied in both acidic and slightly basic environments. After 24h, the percentage of release was, respectively, 50% and 32%. This behaviour, where the loaded NCs do not completely release the encapsulated drug in similar experimental conditions, has already been reported [11, 20]. The carboxylic groups of PMAA are the key for the interpretation of these results [12]. They are mostly protonated at pH 4.0 and they cannot interact with the positively charged CTP complex, causing the release [4].

The results of our *in vitro* DNR release study clearly show, similarly to CTP, that the amount of drug delivered depends on the pH level. This behaviour can be explained by considering the interaction between DNR and the carboxylic groups of the NCs. At physiological pH (≈ 7.4) the carboxylic groups of PMAA are deprotonated and interact with the protonated amino group of DNR, favoring the retention of the drug in the NCs (also encapsulation conditions). At pH 5.5, a lower percentage of carboxylic groups are protonated, which causes a decrease in the number of interactions DDS-DNR and, as a consequence, a larger amount of drug is released. At pH 4.0 the majority of the carboxylic groups are protonated, therefore there will be fewer electrostatic interactions and the drug will be more easily released than in the two previously-described conditions. For more details on these experiments, we refer the reader to the supplementary material S.1, S.2, S.3.

3.2.2. Parameter Identification

The results of our parameter identification procedure are detailed in Tables 3–4 for DNR and CTP, respectively. For DNR we **report** an increase in the value of four of the non-dimensional parameters (D , Da , \tilde{S} and \tilde{k}) with increasing pH, over the values of pH studied in the experiments (Fig. 4). Similar trends are observed for CTP for the parameters D , Da and \tilde{k} , **while** the normalised solubility \tilde{S} decreases with increasing pH (Fig. 4). The value of \tilde{B}_1 , as the initial drug concentration in the shell normalised by the initial concentration in the core, is a function of the fabrication process and remains constant with pH.

An interesting result from Tables 3-4 is the monotonicity of the parameters with pH. The order

Table 3: Optimal nondimensional parameters at three values of pH for DNR.

	Parameter	pH=4	pH=5.5	pH=7.4
1	D	35.60	61.50	113.05
2	Da	0.63	0.96	1.10
3	\tilde{S}	2.64	3.35	5.60
4	\tilde{k}	0.47	4.65	10.89
5	\tilde{B}_1	0.12	0.12	0.12

Table 4: Optimal nondimensional parameters at two values of pH for CTP.

	Parameter	pH=4	pH=7.4
1	D	48.59	86.91
2	Da	0.14	0.67
3	\tilde{S}	2.20	0.11
4	\tilde{k}	0.09	6.31
5	\tilde{B}_1	0.18	0.18

of magnitude of the parameters for DNR and CTP is the same: due to the extremely large space of parameters, this is an indirect confirmation of the correctness of the optimization procedure.

In Figures 5-6 the experimental drug release data for DNR and CTP are shown. The curves correspond to the cumulative percentage of mass released (eqn (2.8)) obtained with the optimal parameters for the values of pH studied. Clearly, the release of each drug is well-captured by the two-phase two-layer dissolution-diffusion-reaction model that we have devised. Probing further, we are able to establish that the slower release of DNR with increasing pH is likely as a result of a slower diffusion coefficient in the shell, coupled with faster binding to components of the shell. As a result, as the pH is increased, a greater fraction of the initial drug load is permanently retained and never released. For CTP, the picture is a little more complicated. Firstly, the decrease in solubility with pH has the effect of slowing the dissolution process. However, there is a modest increase in diffusion coefficient within the shell with pH, which coupled with the simultaneous increase in binding results in a \tilde{k} that greatly exceeds 1, indicating that binding is dominating and transport within the shell is increasingly diffusion-limited.

Our mechanistic model confirms a pH-responsiveness of the PMAA shell in a manner that is dependent on the particular drug studied. For DNR we observe an increasingly pronounced delay in release with pH, likely corresponding to the slower diffusion coefficient and faster binding in the shell with pH, as described above. This effect is significantly less for CTP, where we observe an “initial burst” of drug, particularly for the lowest value of pH, which may be beneficial when a rapid delivery, rather than a delayed and sustained release, is desired. The implication is that, while for targeting cancer the biological effect of the drug is important, the release kinetics of different drugs can vary, meaning that both aspects have to be considered hand-in-hand when

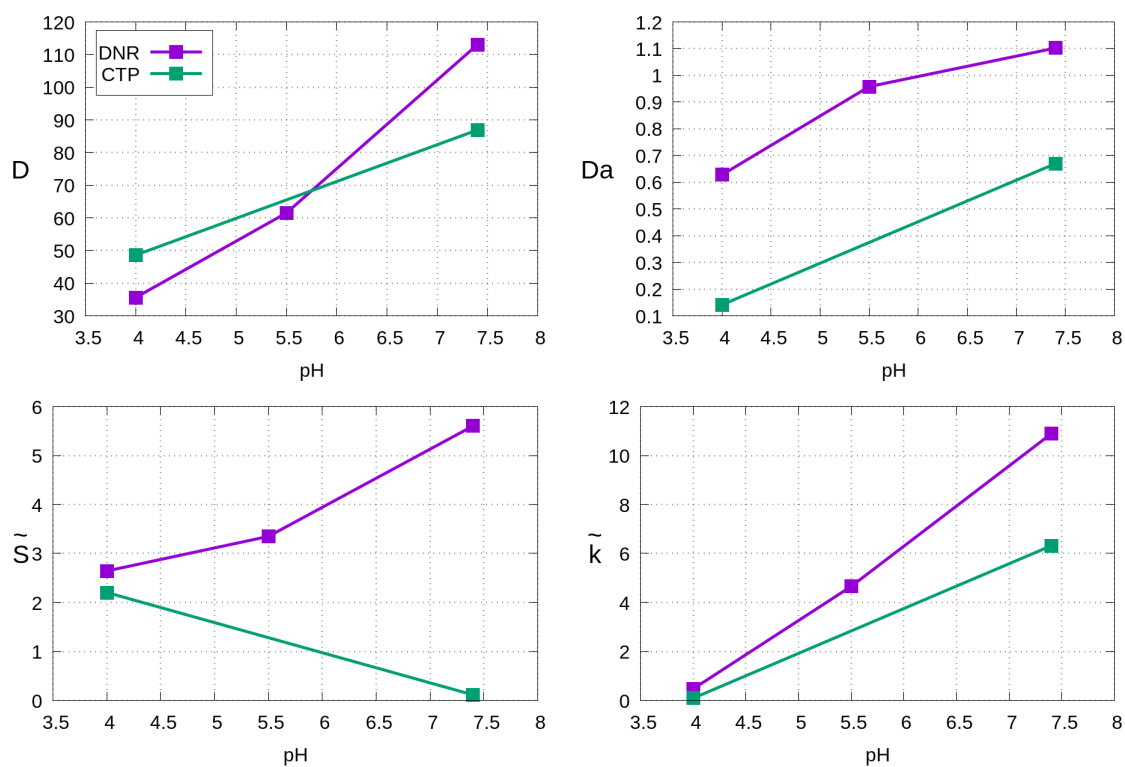


Figure 4: Variation of the four nondimensional parameters D , Da , \tilde{S} , \tilde{k} vs. pH. The initial ratio of concentrations \tilde{B}_1 remains constant with pH.

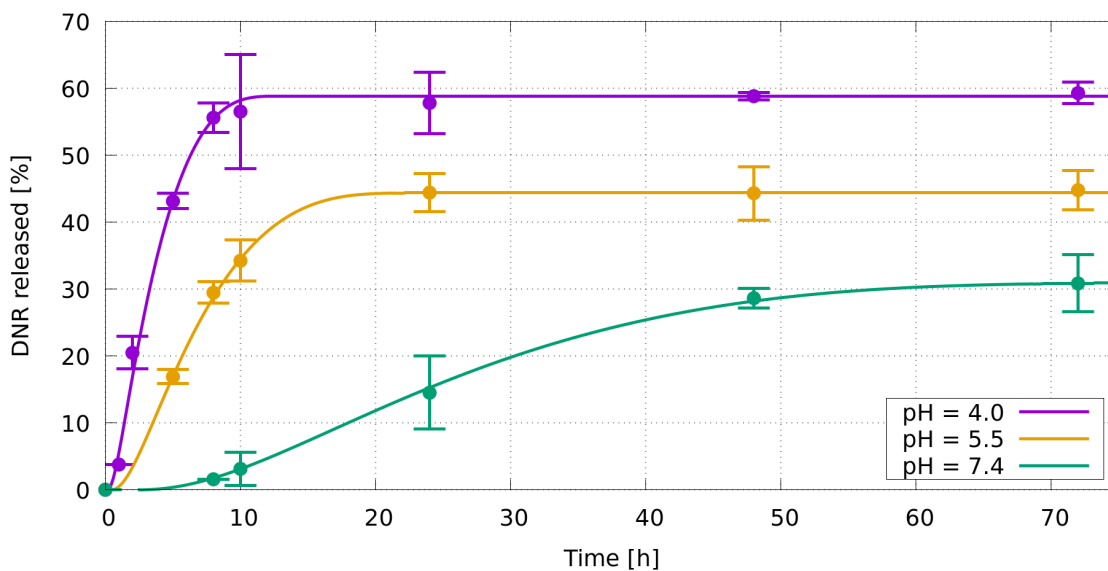


Figure 5: Best fitting release curves vs. experimental data for DNR at pH=4, 5.5 and 7.4.

choosing an appropriate drug to load the NC.

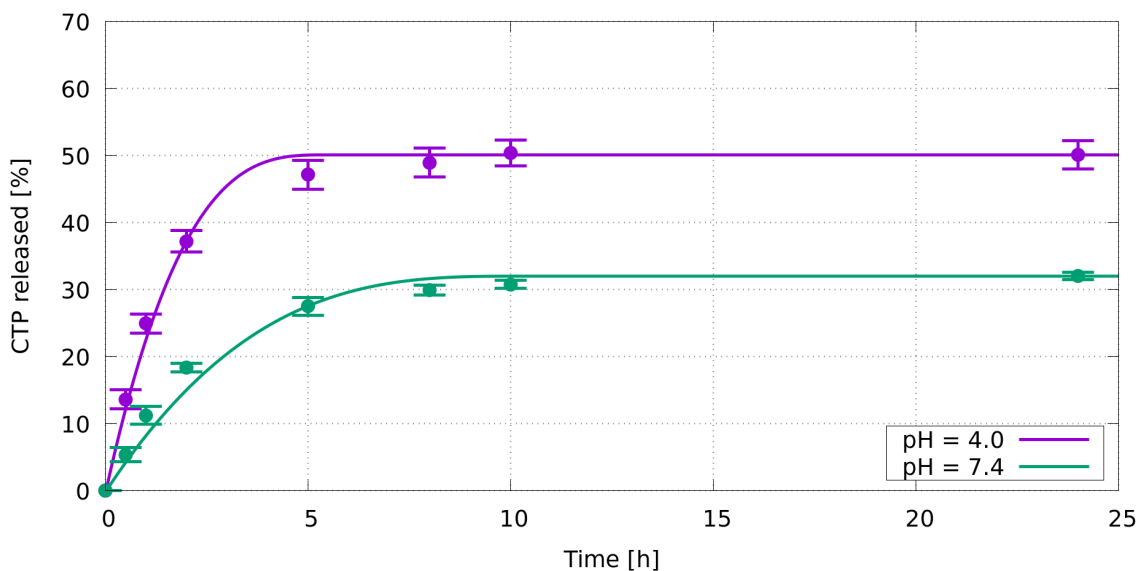


Figure 6: Best fitting release curves vs. experimental data for CTP at pH=4 and 7.4. (experimental data taken from [12]).

4. Limitations

We emphasize that there are limitations in this work. The mathematical model makes a number of assumptions as detailed in the text and the experimental data have been obtained in an *in vitro* environment. Importantly, while we have demonstrated that a dissolution-diffusion-reaction mechanism captures experimental release data, the different identified model parameters for different values of pH points to a complex relationship between pH and the various drug-transport parameters. In this preliminary study, we have not sought to identify the particular functional dependence of the various parameters on pH, for which a more extensive experimental data set would be required, and this is left for future work. Notwithstanding, the approach adopted here of identifying these parameters computationally on a small set of *in vitro* data is still very useful since, once calibrated, the model can be used in a predictive sense to reduce the number of *in vitro* experiments, and with further modifications, can be correlated with *in vivo* data.

5. Conclusions

Nanocontainers made of pH-responsive polymers show great potential in biomedical applications by providing significant advantages over more traditional therapies, both in terms of efficacy and of safety. In particular, their multi-layer structure and ability to encapsulate a wide range of chemicals offers a potential to tailor drug release for the desired application.

We have shown that a pH-responsive drug releasing NC is well described by a dissolution-diffusion-reaction core-shell mechanistic model. Our model is characterized by a biphasic two-layer system: two equations describe the drug dissolution-diffusion in the core, and the other two

equations account for diffusion and pH-dependent reaction with polymer in the shell. Through a sensitivity analysis, the role of various parameters has been demonstrated and, making use of *in vitro* experimental data sets, we have been able to inversely estimate the best-fitting parameters of the model for each pH studied. The different physico-chemical characteristics of the two drugs considered in our case study affect their interactions with the pH-sensitive NCs that in turn, influences the release performance. This is reflected through the parameters of the mathematical model. Once these parameters have been computationally identified, the proposed methodology offers a cheap and useful tool that can be used to quantitatively characterize the drug kinetics, improve the technological performance and optimize the release rate for the target application. The results of current study warrant further investigation with specific *in vivo* therapeutic applications.

Acknowledgments

Funding from the European Research Council under the European Unions Horizon 2020 Framework Programme (No. FP/2014-2020)/ERC Grant Agreement No. 739964 (COPMAT) is acknowledged.

C.C.and G.T. acknowledge funding from the Marie Skodowska-Curie Innovative Training Network (ITN) ClickGene (H2020-MSCA-ITN-2014-642023).

This work is also partially supported by Italian MIUR (PRIN 2017 project: Mathematics of active materials: from mechanobiology to smart devices, project n. 2017KL4EF3).

Supplementary material

S.1. Synthesis of pH-responsive nanocontainers

The synthesis of the pH-responsive NCs has already been reported elsewhere [12]. The pH-sensitive hollow NC are predominantly made of MAA, the monomer responsible for the pH sensitivity due to their carboxylic groups. These can be protonated or deprotonated depending on the pH, enabling different interactions with the external environment [37, 38]. To form the shell, we utilised two additional monomers: N,N-methylenebis(acrylamide) (MBA), used as a cross-linking agent to maintain the structure of the hollow NCs in water, and poly(ethylene glycol) methyl ether methacrylate (PEGMA), which is a hydrophilic, nontoxic component known to show resistance against nonspecific protein adsorption and to prolong the *in vivo* residence time of the DDS [39].

The resulting diameters of the central cavity and of the whole NC suspended in water were $0.3\mu\text{m}$ and $0.55\mu\text{m}$, respectively, according to the requirements for such systems. A relatively constant diameter after long-term storage at room temperature was observed, indicating favorable stability properties. No effects of erosion or degradation were reported over the time scale considered.

S.2. Drug loading

We study the drug-encapsulation and release properties of the pH-sensitive system with two different drugs: DNR (results reported here for the first time) and CTP (already published)[12] (fig. 7). For DNR loading, 5mg of hollow NCs were suspended in 5ml of phosphate buffer saline (PBS, pH 7.4) with the aid of ultrasonic bathing. 5mg of daunorubicin hydrochloride (DNR HCl) were then dissolved in the medium. The suspension was covered with foil and maintained under gentle agitation for 72h at r.t. The non-encapsulated DNR was then removed with 15 cycles of centrifugation/resuspension ($5\text{min} \times 9000\text{rpm}$). The encapsulated amount of DNR was indirectly determined by UV spectroscopy: the total amount of loaded DNR was computed as the difference between the amount of DNR in feeding and in the supernatant fractions. These calculations were based on a standard curve of DNR in PBS and the concentration was determined with absorbance measurements at 484nm. The drug loading process was evaluated using the parameters encapsulation efficiency (EE%) and loading capacity (LC%), defined respectively as:

$$\text{EE\%} = \frac{\text{Encapsulated drug (mg)}}{\text{drug in feeding (mg)}} \times 100$$

$$\text{LC\%} = \frac{\text{Encapsulated drug (mg)}}{\text{drug loaded into NCs (mg)}} \times 100$$

For DNR, we obtained $\text{EE\%} = 87.1 \pm 2.9$ and $\text{LC\%} = 47.2 \pm 0.1$, which translates into an encapsulation of 0.893mg of DNR per 1mg of NC. The loading ability of the hollow NCs relies on the interactions between the groups of the shell and the drug. Specifically, electrostatic interaction is the most important one and involves the negatively charged carboxylic groups of PMAA (in the anionic form $-\text{COO}^-$ in the loading conditions) and the amino groups of the drug (mostly as $-\text{NH}^{3+}$ in the loading conditions).

For CTP loading, 1 mg of NCs was suspended in 950 mL of PBS with the aid of ultrasonic bathing. 2 mg of CTP previously solubilized in 50 mL of ACN were then added to the suspension. The final loading medium, containing 1 mg of NCs and 2 mg of CTP in 1 mL of mixture of

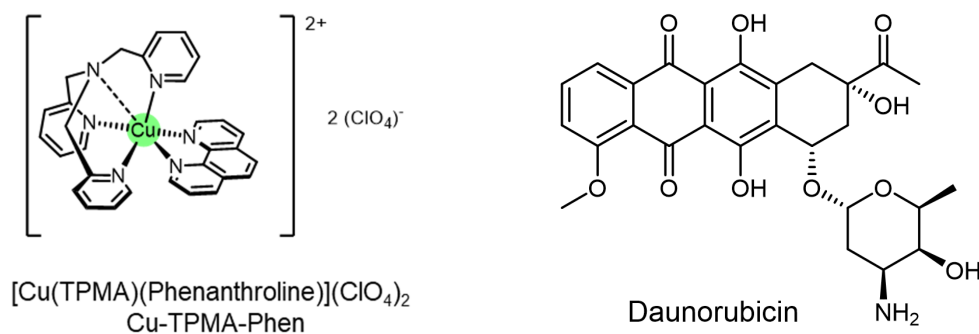


Figure 7: Chemical structure of Cu-TPMA-Phen (CTP) (left) and daunorubicin (DNR) (right).

PBS/ACN 5% v/v, was kept under gentle magnetic stirring for 24h at r.t. The non-encapsulated portion of CTP was removed with five cycles of centrifugations and resuspensions in a fresh mixture PBS/ACN (5 min \times 11000 rpm). The amount of encapsulated CTP was indirectly determined by UV spectroscopy and calculated by the difference of concentration between the original CTP solution and the supernatants containing the non-encapsulated drug. The calculations were based on a calibration curve of CTP obtained in the same solvent mixtures with absorbance measurements at 262 nm [12].

The encapsulation process of CTP resulted in encapsulation efficiency and loading capacity of $EE\% = 36.4 \pm 5.2$ and $LC\% = 42.0 \pm 3.3$, respectively, which corresponds to the encapsulation of 0.724 mg (0.988 μ mol) of CTP per 1mg of NC [12]. Differently from DNR, CTP is water-insoluble and adequate aqueous conditions to dissolve the drug and to suspend the NCs were required. This was achieved by adding 5% of acetonitrile to the loading buffer, i.e. PBS. The main interaction involved in the encapsulation of CTP is probably electrostatic between the negatively charged carboxylate anions of PMAA and the positive charge of Cu.

S.3. *In vitro* drug release studies

The pH sensitivity of the system was tested by means of *in vitro* drug release experiments. For the DNR experiments, 1mg of DNR-loaded NCs were suspended in 0.5ml of buffer and loaded into MWCO 140 kDa dialysis tube and incubated in 50ml each buffer solution. Three different pH conditions were used for the analysis of release: citrate buffer 0.1M pH 4.0; citrate buffer 0.1M pH 6.0 and PBS pH 7.4. At different time points (30min, 1h, 2h, 5h, 8h, 10h, 24h, 48h, 72h), 1ml of the solutions was withdrawn and analyzed. The concentration of each sample, and therefore of the release medium at each time point was determined with UV spectroscopy by using the standard curve method (at 484 nm). A standard curve of DNR was recorded in each buffer used as a release medium.

For CTP *in vitro* drug release study, 1 mg of CTP-loaded NCs was suspended in distilled water, split into two dialysis bags, and incubated in 25 mL of each release medium: citrate buffer 0.1M + 5% ACN pH4.0 and PBS + 5% ACN pH 7.4. At different time points (as above for DNR), 1 mL was collected from each solution and the concentration of the samples was measured using UV spectroscopy. The calculations were made upon a calibration curve of CTP recorded in each buffer (at 262 nm). All experiments were carried out three times for statistical analysis [12].

References

- [1] V. Balamuralidhara, T.M. Pramodkumar et al., pH-sensitive drug delivery systems: a review, *Am. J. Drug Discov. Develop.* 1, 24–28, 2011.
- [2] M.J. Mitchell, M.M. Billingsley, R.M. Haley, M.E. Wechsler, N.A. Peppas, R. Langer, Engineering precision nanoparticles for drug delivery, *Nature Rev. Drug Discovery*, online, 2020.
- [3] M. Matsusaki, M. Akashi, Functional multilayered capsules for targeting and local drug delivery, *Exp. Opin. Drug Deliv.* 6, 1207–1217, 2009.
- [4] X. Yang, L. Chen, B. Huang, F. Bai b, X. Yang, Synthesis of pH-sensitive hollow polymer microspheres and their application as drug carriers, *Polymer*, 50(15), 3556–3563, 2009.
- [5] M. Mahdavi, F. Rahmani, S. Nouranian, Molecular simulation of pH-dependent diffusion, loading, and release of doxorubicin in graphene and graphene oxide drug delivery systems, *J. Mater. Chem. B*, 4, 7441–7451, 2016.
- [6] R.D. Manga, P.K. Jha, Mathematical Models for Controlled Drug Release Through pH-Responsive Polymeric Hydrogels, *J. Pharm. Sci.*, 106, 629–639, 2017.
- [7] J. Varshosaz, M. Falamarzian, Drug diffusion mechanism through pH-sensitive hydrophobic/polyelectrolyte hydrogel membranes, *Euro. J. Pharm. Biopharm.*, 51, 235–240, 2001.
- [8] Y. Xu, Y. Jia, Z. Wang, Z. Wang, Mathematical Modeling and Finite Element Simulation of Slow Release of Drugs Using Hydrogels as Carriers with Various Drug Concentration Distributions, *J. Pharm. Sci.*, 102(5), 1532–1543, 2013.
- [9] Q. Zhao, B. Li, pH-controlled drug loading and release from biodegradable microcapsules, *Nanomedicine: Nanotechnology, Biology, and Medicine* 4, 302–310, 2008.
- [10] D.A. Bedoya, F. N. Figueroa, M.A. Macchione, M.C. Strumia, Stimuli-Responsive Polymeric Systems for Smart Drug Delivery, in *Advanced Biopolymeric Systems for Drug Delivery*, 115–134, Springer, 2020.
- [11] G. Toniolo, E.K. Efthimiadou, G. Kordas, C. Chatgialloglu, Development of multi-layered and multi-sensitive polymeric nanocontainers for cancer therapy: *in vitro* evaluation, *Sci. Rep.* 8, 14704, 2018.
- [12] G. Toniolo, M. Louka, G. Menounou, N.Z. Fantoni, G. Mitrikas, E.K. Efthimiadou, A. Masi, M. Bortolotti, L. Polito, A. Bolognesi, A. Kellett, C. Ferreri, C. Chatgialloglu, [Cu(TPMA)(Phenantroline)](*ClO*₄)₂: Metallodrug Nanocontainer Delivery and Membrane Lipidomics of a Neuroblastoma Cell Line Coupled with a Liposome Biomimetic Model Focusing on Fatty Acid Reactivity, *ACS Omega*, 3, 15952–15965, 2018.
- [13] J. Song, Y. Wei, J. Hu, G. Liu, et. al, pH-Responsive Porous Nanocapsules for Controlled Release, *Chem. Eur. J.*, 24, 212–221, 2018.

- [14] J. Majumder, T. Minko, Multifunctional and stimuli-responsive nanocarriers for targeted therapeutic delivery, *Exp. Opin. Drug Deliv.*, online, 2020.
- [15] L. Palanikumar, S. Al-Hosani, M. Kalmouni, et al., pH-responsive high stability polymeric nanoparticles for targeted delivery of anticancer therapeutics, *Comm. Biology*, 3(95), 2020.
- [16] N. Deirram, C. Zhang, S. S. Kermaniyan, et al., pH-Responsive Polymer Nanoparticles for Drug Delivery, *Macromol. Rapid Commun.* 40, 1800917, 2019.
- [17] Juan Liu, Y. Huang, A. Kumar et. al, pH-Sensitive nano-systems for drug delivery in cancer therapy, *Biotech. Adv.*, 32, 693–710, 2014.
- [18] X. Zhang, Y. Lin, R. J. Gillies, Tumor pH and its measurement, *J. Nucl. Med.* 51 (8), 1167–70, 2010.
- [19] Y. Jiang, N. Krishnan, J. Zhou, S. Chekuri, Dr. X. Wei, Dr. A. V. Kroll, C. L. Yu, Y. Duan, Dr. W. Gao, R. H. Fang, L. Zhang, Engineered Cell-Membrane-Coated Nanoparticles Directly Present Tumor Antigens to Promote Anticancer Immunity, *Adv. Mater.*, 32, 2001808, 2020.
- [20] X.J. Kang, Y.L. Dai, P.A. Ma, D.M. Yang, C.X. Li, Z.Y. Hou, Z.Y. Cheng, J. Lin, Poly(acrylic acid)-modified Fe₃O₄ microspheres for magnetic-targeted and pH-triggered anticancer drug delivery, *Chem. Eur. J.*, 18, 15676–15682, 2012.
- [21] J. Siepmann, F. Siepmann, Modelling of diffusion controlled drug delivery, *J. Contr. Release*, 161 (2012) 351–362.
- [22] T. Higuchi, Rate of release of medicaments from ointments bases containing drugs in suspension. *J. Pharm. Sci.*, 50(10), 874–875, 1961.
- [23] P.L. Ritger, N.A. Peppas, A simple equation for describing of solute release. I. Fickian and non-Fickian release from non-swelling devices in the form of slabs, spheres, cylinders or discs, *J. Contr. Release*, 5, 23–36, 1987.
- [24] R.W. Korsmeyer, R. Gurny, E.M. Doelker, P. Buri, N.A. Peppas, Mechanism of solute release from porous hydrophilic polymers, *Int. J. Pharmaceutics*, 15, 25–35, 1983.
- [25] Y. Wang, K. Zhang, X. Qin et al., Biomimetic nanotherapies: red blood cell based core-shell structured nanocomplexes for atherosclerosis management, *Adv. Science*, 1900172, 2019.
- [26] M. Grassi, G. Lamberti, S. Cascone, G. Grassi, Mathematical modeling of simultaneous drug release and in vivo absorption, *Int. J. Pharm.*, 418, 130141, 2011.
- [27] S. McGinty, G. Pontrelli, A general model of coupled drug release and tissue absorption for drug delivery devices, *J. Contr. Release*, 217, 327-336, 2015.
- [28] G. Frenning, Theoretical investigation of drug release from planar matrix systems: effects of a finite dissolution rate, *J. Contr. Release*, 92, 331–339, 2003.

- [29] S. McGinty, S. McKee, R.M. Wadsworth, C. McCormick, Modelling drug-eluting stents, *Math. Med. Biol.* 29 (1), 1–29, 2011.
- [30] D. Peri, E.F. Campana, High-Fidelity Models in Global Optimization, *Lecture Notes in Computer Science book series (LNCS)*, 3478, 112–126, 2005.
- [31] R.B. Statnikov, J.B. Matusov, Use of P_τ Nets for the Approximation of the Edgeworth-Pareto Set in Multicriteria Optimization, *J. Optim. Theory Appl.*, 91 (3), 543–560, 1996.
- [32] P. D. Hough, T.G. Kolda, V.J. Torkzgon, Asynchronous parallel pattern search for nonlinear optimization, *SIAM J. Sci. Comput.*, 23 (1), 134–156, 2001.
- [33] E. Fleige, M.A. Quadir, R. Haag, Stimuli-responsive polymeric nanocarriers for the controlled transport of active compounds: Concepts and applications, *Adv. Drug Deliv. Rev.*, 64, 866–884, 2012.
- [34] S. Ganta, H. Devalapally, A. Shahiwala, M. Amiji, A review of stimuli-responsive nanocarriers for drug and gene delivery, *J. Contr. Release*, 126, 187–204, 2008.
- [35] E.K. Efthimiadou, M. Theodosiou, G. Toniolo, N.Y. Abu-Thabit, Stimuli-responsive biopolymer nanocarriers for drug delivery applications, in *Stimuli Responsive Polym. Nanocarriers Drug Deliv. Appl. Vol. 1* (Eds.: A.S.H. Makhlof, N.Y. Abu-Thabit), Woodhead Publishing, 405–432, 2018.
- [36] N. Zuin Fantoni, Z. Molphy, C. Slator, G. Menounou, G. Toniolo, G. Mitrikas, V. McKee, C. Chatgililoglu, A. Kellett, Polypyridyl-based Copper Phenanthrene Complexes: A New Type of Stabilized Artificial Chemical Nuclease, *Chem. Eur. J.*, 25(1), 221–237, 2019.
- [37] Y. Qiu, K. Park, Environment-sensitive hydrogels for drug delivery, *Adv. Drug Deliv. Rev.*, 64, 49–60, 2012.
- [38] K. Zhang, Y. Luo, Z. Li, Synthesis and Characterization of a pH- and Ionic Strength-Responsive Hydrogel, *J. Soft Mater.*, 5, 183–195, 2007.
- [39] P. Bilalis, N. Boukos, G.C. Kordas, Novel PEGylated pH-sensitive polymeric hollow microspheres, *Mater. Lett.*, 67, 180–183, 2012.
- [40] R. Kiraly, R.B. Martin, Metal ion binding to daunorubicin and quinizarin, *Inorganica Chim. Acta*, 67, 13–18, 1982.